ISSN 1027-4510, Journal of Surface Investigation. X-ray, Synchrotron and Neutron Techniques, 2013, Vol. 7, No. 5, pp. 825–832. © Pleiades Publishing, Ltd., 2013.
Original Russian Text © E.V. Emelin, L.S. Kokhanchik, M.N. Palatnikov, 2013, published in Poverkhnost'. Rentgenovskie, Sinkhrotronnye i Neitronnye Issledovaniya, 2013, No. 9, pp. 19–26.

Periodic Domain Structures in Stoichiometric Lithium Niobate: Formation by Electron Beam

E. V. Emelin[a], L. S. Kokhanchik[a], and M. N. Palatnikov[b]

[a] *Institute of Microelectronics Technology and High Purity Materials, Russian Academy of Sciences, Chernogolovka, Moscow oblast, Russia*

[b] *Institute of Chemistry and Technology of Rare Elements and Mineral Raw Materials, Russian Academy of Sciences, Apatity, Murmansk oblast, Russia*

e-mail: mlk@iptm.ru

Received April 15, 2013

Abstract—The formation of periodic domain structures in stoichiometric lithium niobate crystals via direct surface irradiation using a controllable electron beam in a scanning electron microscope is studied. The periodic domain structures are fabricated at different microscope parameters (current, voltage, charge density) and different ways of charge implantation. The irradiation modes for the formation of uniform periodic domain structures are experimentally found. The use of optimal electron-beam parameters and ways of crystal surface irradiation make it possible to fabricate domain structures with a period of 6.9 μm in a crystal 0.5 mm thick. Domain structures of this kind can be used for optical wavelength conversion by quasi-phase-matching and second harmonic generation in lithium niobate.

DOI: 10.1134/S102745101305008X

INTRODUCTION

Ferroelectric domain structures with the given configuration are a promising nonlinear medium for transformation of the laser radiation frequency and implementation of other possibilities of controlling its parameters. Transformation of the radiation into the second harmonic (SH) at regular or periodic domain structures created in a $LiNbO_3$ crystal possessing such necessary qualities as high quadratic nonlinear susceptibility and stability of domain structures created by different methods was demonstrated in [1]. The periods of domain structures in $LiNbO_3$ crystals necessary for transformation into SH radiation of the near-infrared (IR) and visible ranges are within 3–18 μm [2]. The direct electron-beam repolarization method has a series of advantages over the after-growth methods of the formation of such a type of structures (the field method [3], metal probe [4], and laser radiation [5]). The main advantage is the possibility of forming domain structures of arbitrary shape on large surface areas in a rather short time, the lack of special masks and coatings, and also the possibility of varying the irradiation parameters within a wide range. The development and improvement of the direct electron-beam repolarization method of Z cuts of a $LiNbO_3$ crystal of congruent composition were considered in [6–9].

Lithium niobate has a wide range of homogeneity on the phase diagram and is a phase of variable composition that makes it possible grow nominally pure single crystals with different ratios $R = [Li_2O]/[Nb_2O_5]$ and, respectively, with different defect structures and different physical and optical properties [10]. Of most practical (commercial) importance is the composition grown from congruent melt with the ratio $R = [Li_2O]/[Nb_2O_5] = 0.946$. The main drawback of crystals of this composition limiting their use in nonlinear optics is the relatively low beam stability [11]. Lithium niobate crystals grown from a congruent composition possess a high coercive field ($E_c = 220 \times 10^3$ V/cm) and spontaneous polarization $P_s = 71$ μC/cm^2 [10].

The stoichiometric composition of lithium niobate ($R = [Li_2O]/[Nb_2O_5] = 1$) has higher beam stability [11] but these crystals have not found wide practical application because of their insufficient optical homogeneity. In comparison with crystals grown from a congruent composition, single crystals of stoichiometric composition have significant advantages when creating nonlinear laser media with periodically polarized structures, since the induced electric field sufficient for switching the spontaneous polarization in these crystals is much lower (by a factor of 4–5 and more) [12]. Nondestructive methods for controlling the degree of stoichiometry of $LiNbO_3$ are measurements of the UV edge of intrinsic absorption [13] and measurements of the Raman spectra [14].

In this work, we study the effect of the irradiation parameters (accelerating voltage, electron-beam cur-

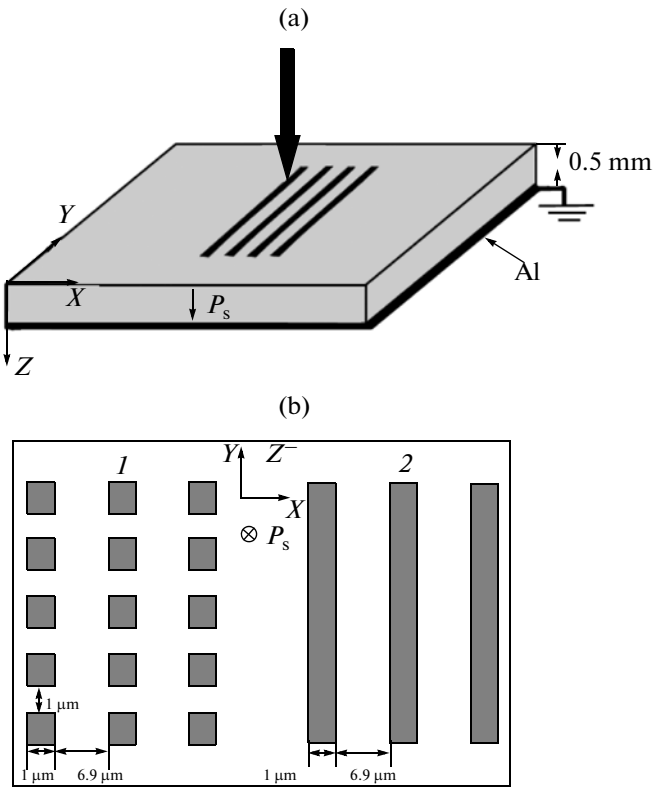

Fig. 1. Scheme of irradiation with the electron beam: (a) total scheme of irradiation with the electron beam in the sample; (b) (*1*) discrete charge implantation with the interval 1 μm and (*2*) continuous irradiation along the line of the given size.

rent, charge density), and also the effect of different methods of the implantation of charge carriers into the sample surface layer, on the quality and uniformity of the formation of periodic domain structures (PDSs) in a $LiNbO_3$ crystal of stoichiometric composition. This work is aimed at finding the optimum conditions for the formation of uniform PDSs by a focused electron beam upon irradiation of the surface of negative (Z^-) cuts of stoichiometric lithium-niobate crystals.

EXPERIMENTAL

A $LiNbO_3$ crystal of stoichiometric composition was grown by the Czochralski method using a Kristall-2 setup from melt enriched with Li_2O (~58.6 mol % Li_2O) [10]. The significant difference in the melt and crystal compositions determined the need to greatly decrease (by several orders of magnitude) the growth rate in comparison with congruent crystals in order to suppress concentration supercooling which leads to noticeable changes in the composition at different stages of the process. Comparative studies of the Raman spectra of the grown stoichiometric lithium-niobate crystals confirm their rather accurate correspondence to the stoichiometric composition ($R = [Li_2O]/[Nb_2O_5] = 1$) [15] by the zero intensity of the spectral line with a frequency of 120 cm^{-1}.

Optically polished samples of Z cuts 0.5 mm thick were used for manufacturing the PDSs. The Z^- cuts, whose spontaneous-polarization P_s vector is directed from the surface inside the sample, were irradiated. The opposite surface (Z^+) was preliminarily coated with a metal (Al) layer with a thickness of ~0.1 μm. The samples were grounded to produce a homogeneous electric field (Fig. 1a).

The domain structures were formed using a Zeiss EVO-50 raster electron microscope equipped with a "NanoMaker" apparatus complex for controlling the electron beam at accelerating voltages of $U = 5$, 15 and 25 kV, an electron beam current of $I = 0.1$–2 nA, an implanted charge density of $D_{irr} = 100$–2000 μC/cm^2. ($D = It_{irr}/S_{irr}$, where I is the current, t_{irr} is the irradiation time, S_{irr} is the irradiated area.)

Charge implantation by the electron beam was performed in two ways (Fig. 1b): (i) the irradiation of discrete regions with an interval of 1 μm; (ii) continuous irradiation of lines with a width of 1 μm by the electron beam. Periodic lines were plotted in the Y and X directions.

Test plotting by the electron beam under the same irradiation modes (U, I) but with different values of the implanted-charge density D_{irr} was performed on neighboring small regions of the surface. The total size of the surface with structures obtained at different D_{irr} and in different ways was ~400 × 400 μm.

Visualization of the domain structures formed by the electron beam was performed after chemical etching of the samples in a $HF + 2HNO_3$ solution for 60 s at a temperature of 110°C. We used a Zeiss Axioplan 2 optical interference microscope. The mode of Nomarski differential interference contrast (DIC) implemented in this microscope makes it possible to strongly improve the contrast even of a very small surface relief.

EXPERIMENTAL RESULTS AND DISCUSSION

The most obvious origin of the appearance of domains during the irradiation of the lithium-niobate Z^- cut with electrons is the space-charge field E_{sc} appearing upon nonequilibrium pumping of the trap levels by the electron beam. Current ideas concerning the formation of the space-charge region and E_{sc} fields in dielectrics under the action of an electron beam are presented in [16–18]. The electric field formed under electron irradiation of the polar Z^- cut is directed opposite to the vector P_s and when reaching the threshold value which exceeds the coercive field of $LiNbO_3$, it can switch the spontaneous polarization of the crystal [7].

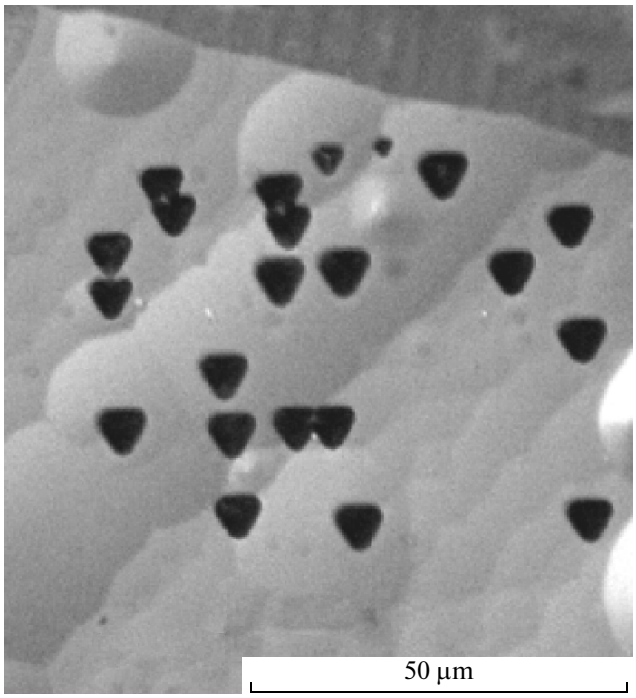

Fig. 2. Single domains on the Z^--surface of $LiNbO_3$ at $U = 5$ kV, $I = 0.5$ nA, $D_{irr} = 1500$ μC/cm^2.

The electron penetration depth R_e in the sample at different energy values was estimated according to the formula [19]:

$$R_e = 78.9U^{1.7}/\rho,$$

where $\rho = 4.65$ g/cm^3 is the density of $LiNbO_3$; according to the estimates, R_e varies from several hundreds of nanometers at $U = 5$ kV to ~4 μm at $U =$ 25 kV. Thus, the electron penetration depth increases considerably when the accelerating voltage increases. Consequently, the depth of the generation of domains depends on the primary energy of the electrons irradiating the surface.

Figure 2 shows single triangular domains with a size of ~4–5 μm formed at an accelerating voltage of $U =$ 5 kV. The domains emerged in arbitrary regions of the irradiation area, and PDSs were not formed. The threshold value of the charge contributed by the electron beam necessary for the formation of domains at 5 kV was estimated disregarding the fraction of reflected and secondary electrons and was ~$(1–1.5) \times 10^{-11}$ C, which corresponds to D_{irr} ~ 1000–1500 μC/cm^2. The domains formed at 5 kV did not grow to reach the opposite side of the sample.

The experiments on the formation of domains by an electron beam at $U = 15$, 25 kV demonstrated that single domains began to form in the irradiated regions with an implanted-charge dose an order of magnitude less than that at 5 kV. The first individual domains were recorded at $D_{irr} = 100$ μC/cm^2. It is obvious that upon deeper electron penetration the field of trapped charges E_{sc} reaches threshold values faster ($E_{sc} > E_c$) than at 5 kV. This can be explained by a decrease in the effect of the surface conductivity on the rate of charge accumulation and a decrease in secondary-electron emission at high electron energies [20]. Consequently, a lower D_{irr} value is needed for the formation of domains at 15 and 25 kV, all other irradiation conditions being equal.

The results of test plotting by the electron beam at $U = 15$ and 25 kV are shown in Fig. 3. Two upper rows of PDSs are formed by continuous irradiation of the surface of the crystal, and two lower rows are formed by discrete irradiation (Fig.1b). Studies of the relief of the Z^-- and Z^+ surfaces of the sample after etching showed that at almost all irradiation mode the domains grew to reach the opposite side. Periodic domain structures began to form at an irradiation dose of $D_{irr} = 300$ μC/cm^2. The stable result of the formation of PDSs was achieved starting from an irradiation dose of $D_{irr} = 500$ μC/cm^2. Analysis of the structures obtained at different combinations (U, I) showed that for the accelerating voltages $U = 15$ and 25 kV the discrete way of charge implantation is characterized by an implicit advantage. During discrete charge implantation in the Y and X directions, uniform domain structures were formed over the entire volume of the crystal from the Z^- to the Z^+ surfaces at almost all values of the electron-beam current starting from $D_{irr} >$ 300 μC/cm^2. In the case of continuous charge implan-

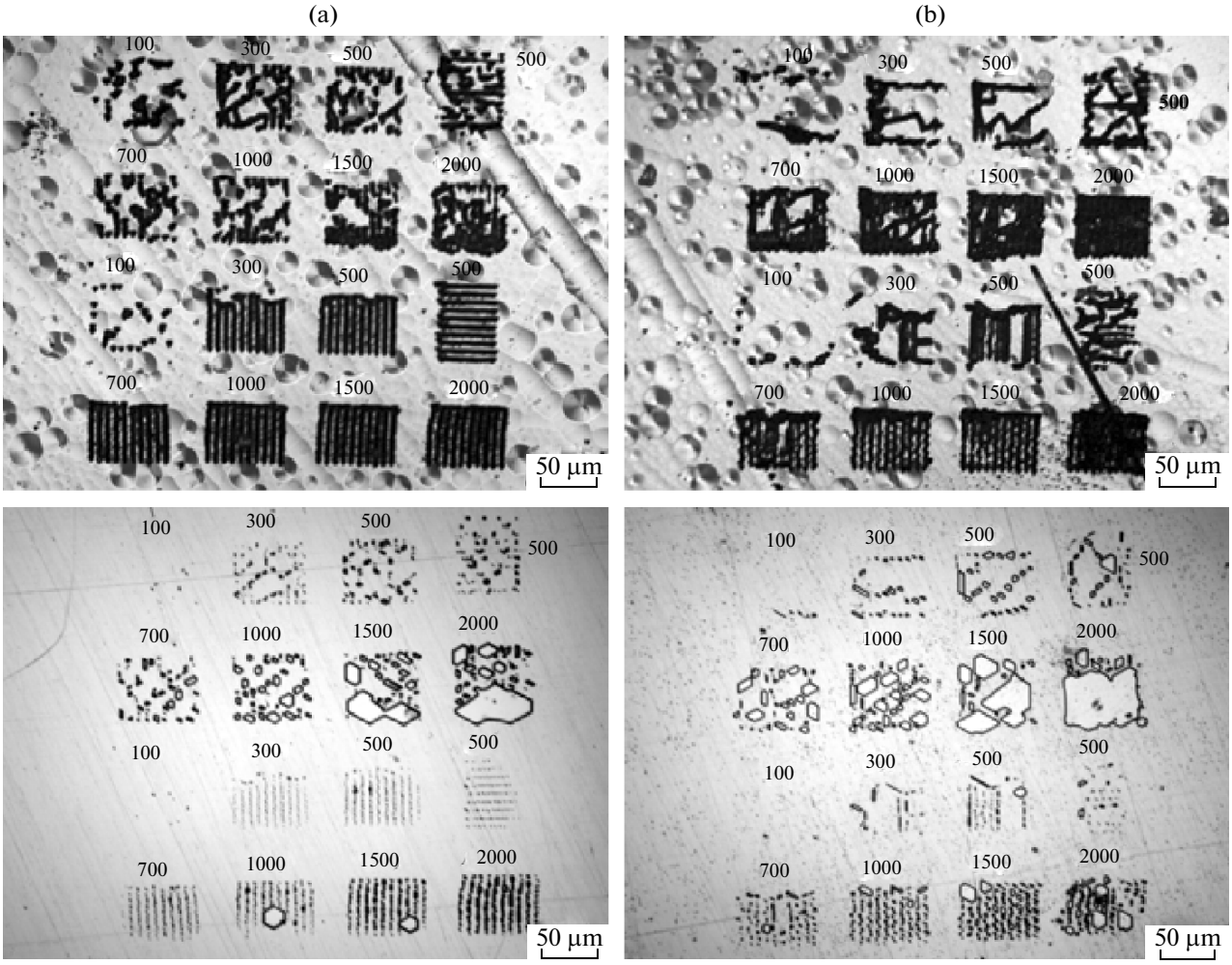

Fig. 3. Domain structures on the Z^-- and Z^+ cuts formed at different implanted-charge densities and electron-beam parameters for the continuous (structures of the two upper rows) and discrete (structures of the two lower rows) ways of charge implantation: (a) $U = 15$ kV, $I = 0.1$ nA, $D_{irr} = 100–2000$ μC/cm^2; (b) $U = 25$ kV, $I = 0.3$ nA, $D_{irr} = 100–2000$ μC/cm^2. The images of the obtained structures are given on the Z^- cut at the top, and on the Z^+ cut at the bottom. The D_{irr} values are specified on the images.

tation, the uniformity and periodicity of the domain structures in the volume was violated. We note that the charge density during continuous implantation, in comparison with the discrete one, almost doubles. It is obvious that this leads to faster charge accumulation in the irradiation area and the formation of higher electric fields. However, the uniformity of the PDSs is broken which is seen well when studying the relief on the Z^+ surface after etching. Consequently, the achievement of field values of $E_{sc} > E_c$ is not the only necessary condition for the formation of uniform domain structures. An important factor for obtaining uniform PDSs is the discrete distribution of the switching fields along line of charge implantation. This is possibly connected with the discreteness of the process of the generation of domains in lithium niobate which is often experimentally observed [21]. Small variations in the intervals (~0.5–1.5 μm) between the irradiated regions also made it possible to form uniform PDSs over the entire volume of the crystal.

Analysis of the obtained PDSs showed that periodic domain structures on the irradiated side consist of domains with a triangular form merging into lines. The width of these lines was ~5 μm. In the case of irradiation of the surface in the Y direction, the triangular domains were located one after another, apex to base. Irradiation of the surface of the crystal along the X direction led to the formation of domain lines with straight and zigzag walls (Fig. 4). The domain structure on the Z^+ surface ($D_{irr} = 500$ μC/cm^2) depends weakly on a change in the crystallographic direction. Because of the narrowing cone-shaped shape of the growing domains, domains with a size of 1–2 μm were arranged with small intervals. The lateral expansion

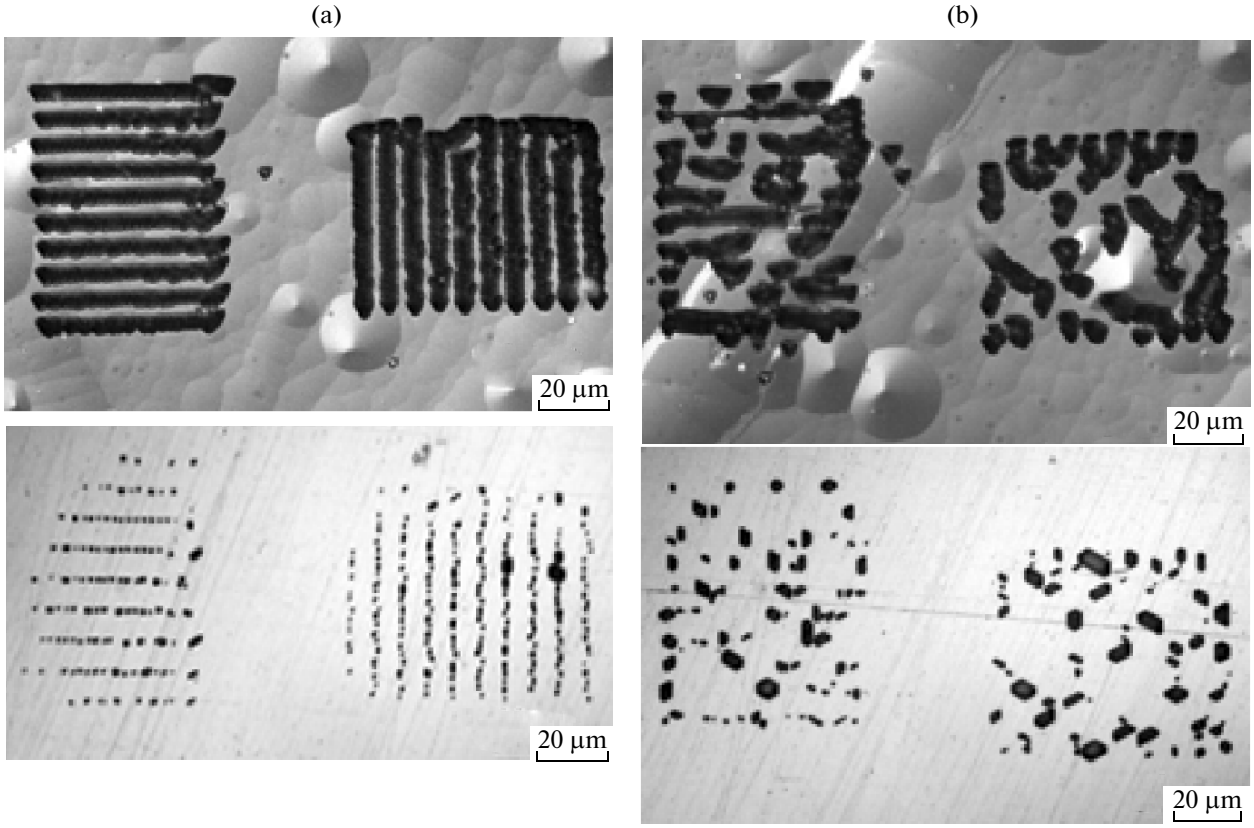

Fig. 4. Domain structures formed as a result of applying different ways of charge implantation at $U = 15$ kV, $I = 0.1$ nA, $D_{irr} = 500$ μC/cm^2: (a) discrete scheme (*1*); (b) continuous scheme (*2*). The upper part shows images for the Z^- cut, the bottom part shows image for the Z^+ cut.

and merging of the domains on the Z^+ surface began at an irradiation dose of $D_{irr} = 700$ μC/cm^2 (Fig. 5). This process started earlier in the case of continuous implantation due to the higher implanted-charge value. The processes of expansion and merging of the domain lines on the Z^+ surface at an accelerating voltage of 25 kV were more intense than those at $U =$ 15 kV, and the structures were inhomogeneous (Fig. 3b). The most favorable mode of the formation of PDSs in stoichiometric crystals corresponded to an accelerating voltage of $U = 15$ kV. Usually irradiation with $U = 25$ kV was used for the $LiNbO_3$ crystal of congruent composition [6–9].

We note that the domain structure on the Z^- surface for both means of charge implantation experiences less changes than on the Z^+ surface with increasing implanted-charge value. The width of the domain lines on the Z^- surface barely changes in comparison with the initial width of ~5 μm. A significant decrease in the value of the switching field occurs far from the irradiation of the cut (Z^-) but the lateral expansion of the domain structures is considerable. The explanation of the observed delay in the lateral expansion of the domains directly on the irradiated surface can be the presence of an excess charge concentration induced by the electron beam. The increased concentration of these charges and the additional electric fields related to them can affect the motion of the domain walls. The expansion of domains can also be affected by the appearance of a double layer of charges due to the emission of secondary electrons from the thin surface layer [16, 17]. The field of the double layer of charges is opposite to the field switching the spontaneous polarization of the crystal. It is possible that this also affects the lateral expansion of domains directly on the irradiated surface. The domain walls in deeper regions of the crystal can move more freely.

The above analysis of domain structures formed by an electron beam made it possible to determine the optimum conditions, which were tested during the formation of PDSs by an electron beam in the region of sizes of 500 × 500 μm. The region of the domain structure with the given period $\Lambda = 6.9$ μm is given in Fig. 6. The etching relief of the Z^- surface corresponded to the continuous periodic lines consisting of merged domains. The domain structure on the Z^+ sur-

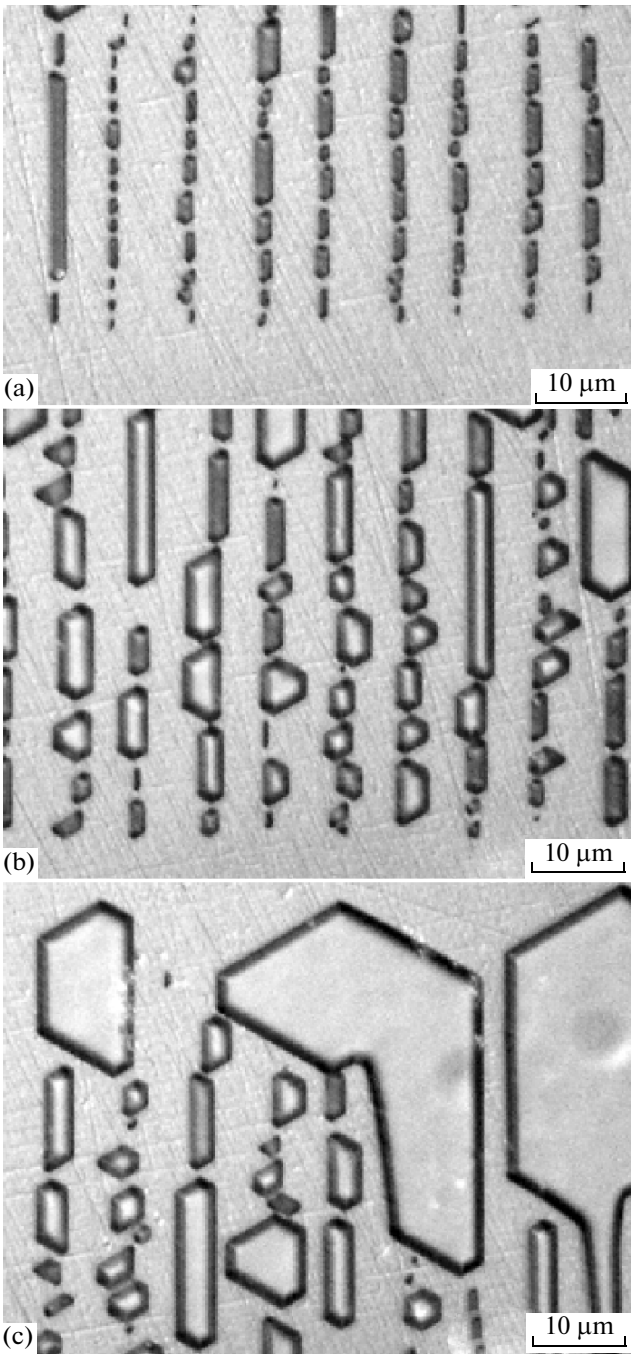

Fig. 5. Domains formed by the discrete way of charge implantation reaching the surface of the Z^+ cut at $U = 15$ kV, $I = 1$ nA and the irradiation dose: (a) $D_{irr} = 700$ μC/cm^2; (b) $D_{irr} = 1500$ μC/cm^2; (c) $D_{irr} = 2000$ μC/cm^2.

face after etching corresponded to the discrete distribution of irradiated areas. In addition, we note that DIC contrast was found in the optical interference microscope on the Z^- surface studied before etching, which corresponded exactly to the distribution of open domains revealed by etching. This result indicates that open domains in the Z cuts of lithium niobate growing from irradiation area may form a small surface relief on the irradiated surface.

CONCLUSIONS

Thus, in this work we studied the process of the formation of PDSs of the bulk type in Z cuts of stoichiometric lithium-niobate crystals by the method of direct electron-beam repolarization. The different irradiation modes and their effect on the character of changes during the formation of domain structures were studied. It was noted that domain structures of the best quality were formed in the stoichiometric

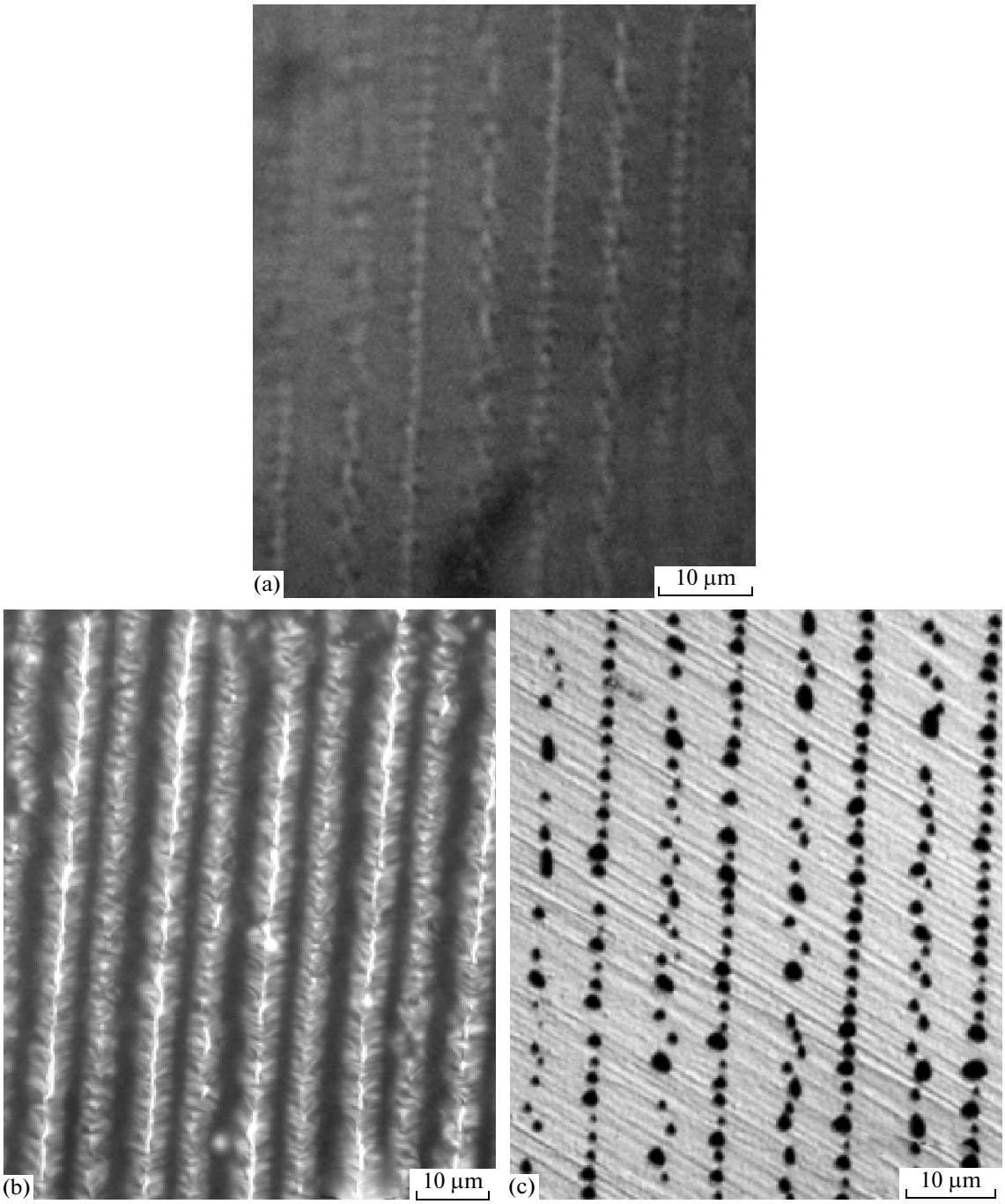

Fig. 6. Region of the periodic domain structure with $\Lambda = 6.9$ μm fabricated by the electron beam on an area of 500 × 500 μm. The optical image in the DIC-contrast mode: (a) polished Z^- surface before chemical etching; (b) Z^- surface after etching; (c) Z^+ surface after etching.

crystal at an accelerating voltage of not 25 kV but 15 kV unlike crystals with congruent composition. Single domains could be formed also at 5 kV. The advantage of discrete charge implantation in comparison with the continuous one was experimentally discovered when the periodic domain structures were fabricated. The optimum parameters of the formation of PDSs by an electron beam with the periods $\Lambda \sim 7$ μm in the crystals with a thickness of 0.5 mm were determined based on the results of the study.

REFERENCES

1. T. Volk and M. Wöhlecke, *Lithium Niobate: Defects, Photorefraction and Ferroelectric Switching* (Springer, Berlin, 2008).

2. Y. L. Lu, Y. Q. Lu, X. F. Cheng, C. C. Xue, and N. B. Ming, Appl. Phys. Lett. **68**, 2781 (1996).
3. H. Ishizuki, I. Shoji, and T. Taira, Appl. Phys. Lett. **82**, 4062 (2003).
4. G. Rosenman, P. Urenski, A. Agronin, Y. Rosenwaks, and M. Molotskii, Appl. Phys. Lett. **82**, 103 (2003).
5. V. Dierolf and C. Sandmann, Appl. Phys. Lett. **84**, 3987 (2004).
6. J. He, S. H. Tang, Y. Q. Qin, P. Dong, H. Z. Zhang, C. H. Kang, W. X. Sun, and Z. X. Shen, J. Appl. Phys. **93**, 9943 (2003).
7. A. Nutt, V. Gopalan, and M. Gupta, Appl. Phys. Lett. **60**, 2828 (1992).
8. C. Restoin, C. Darraud-Taupiac, J. L. Decossas, J. C. Vareille, J. Hauden, and A. Martinez, J. Appl. Phys. **88**, 6665 (2000).
9. Y. Glickman, E. Winebrand, A. Arie, and G. Rosenman, Appl. Phys. Lett. **88**, 011103 (2006).
10. Yu. S. Kuz'minov, *Electrooptical and Nonlinear Optical Lithium Niobate Crystal* (Nauka, Moscow, 1987) [in Russian].
11. A. A. Blistanov, *Crystals for Quantum and Nonlinear Optics* (MISIS, Moscow, 2000) [in Russian].
12. V. Gopalan, T. E. Mitchell, Y. Furukawa, and K. Kitamura, Appl. Phys. Lett. **72**, 1981 (1998).
13. M. Woehlecke, G. Corradi, and K. Betzler, Appl. Phys. B **63**, 323 (1996).
14. N. V. Sidorov, T. R. Volk, B. N. Mavrin, and V. T. Kalinnikov, *Lithium Niobate. Defects, Photorefraction, Vibrational Spectrum, Polaritons* (Nauka, Moscow, 2003) [in Russian].
15. N. V. Sidorov, P. G. Chufyrev, M. N. Palatnikov, and V. T. Kalinnikov, Nano Mikrosist. Tekh., No. 3, 12 (2006).
16. J. Cazaux, J. Appl. Phys. **85**, 1137 (1999).
17. E. I. Rau, E. N. Evstaf'eva, and M. V. Andrianov, Phys. Solid State **50**, 621 (2008).
18. S. Fakhfakh, O. Jbara, S. Rondot, A. Hadjadj, J. M. Patat, and Z. Fakhfakh, J. Appl. Phys. **108**, 093705 (2010).
19. D. B. Wittry and D. F. Kyser, J. Appl. Phys. **38**, 375 (1967).
20. I. M. Bronshtein, and B. S. Fraiman, *Secondary Electron Emission* (Nauka, Moscow, 1969) [in Russian].
21. E. A. Mingaliev, V. Ya. Shur, D. K. Kuznetsov, S. A. Negashev, and A. I. Lobov, Ferroelectrics **399**, 141 (2010).

Translated by L. Mosina